Method for measuring the refractive index distribution of a GRIN lens with heterodyne interferometry

H. C. Hsieh*, Y. L. Chen, W. T. Wu, D. C. Su
Department of Photonics and Institute of Electro-Optical Engineering, National Chiao-Tung University, 1001 Ta-Hsueh Road, Hsinchu 30050, Taiwan, ROC

ABSTRACT

Based on the Fresnel's equations and the heterodyne interferometry, an alternative method for measuring the refractive index distribution of a GRIN lens is presented. A light coming from the heterodyne light source passes through a quarter-wave plate and is incident on the tested GRIN lens. The reflected light passes through an analyzer and an imaging lens; finally it enters a CMOS camera. The interference signals produced by the components of the s- and the p-polarizations are recorded and they are sent to a personal computer to be analyzed. In order to measure the absolute phases of the interference signals accurately, a special condition is chosen. Then, the interference signals become a group of periodic sinusoidal segments, and each segment has an initial phase ψ with the information of the refractive index. Consequently, the estimated data of ψ are substituted into the special equations derived from Fresnel's equations, and the refractive index distribution of the GRIN lens can be obtained. Because of its common-path optical configuration, this method has both merits of the common-path interferometry and the heterodyne interferometry. In addition, the phase can be measured without reference signals.

Keywords: Circular-polarized light, full-field heterodyne interferometry, refractive index , GRIN lens, absolute phase, electro-optic modulator

1. INTRODUCTION

The gradient index (GRIN) lenses have many applications in wide field such as copying machines, optical scanners, fiber optics light coupling systems. To enhance their quality and performance, it is necessary to measure the refractive index distribution of a GRIN lens accurately. Although several techniques [1-5] have been proposed for measuring refractive index, almost all of them are suitable only for one-point measurement. To overcome this drawback, an alternative method for measuring the two-dimensional refractive index distribution of a GRIN lens is presented in this paper based on Fresnel equations [6] and the heterodyne interferometry [7]. Its heterodyne light source (HLS) consists of a linearly polarized laser, an electro-optic modulator (EO) with half-wave voltage V_π, a linear voltage amplifier, and a function generator. The EO is applied with an external sawtooth voltage signal with amplitude V. The light coming from the HLS passes through a quarter-wave plate and is incident on the tested GRIN lens. The reflected light passes through an analyzer and an imaging lens; finally it enters a fast CMOS camera. The interference signals produced by the components of the s- and the p-polarizations are recorded and they are sent to a personal computer to be analyzed. Here the EO acts as a heterodyne phase-shifter [8]. In order to measure the absolute phases of the interference signals accurately, the condition $V_\pi > V > V_\pi/2$ is chosen. The interference signals recorded at each pixel become a group of periodic sinusoidal segments, and each segment has an initial phase ψ with the information of the refractive index. The associated phase of each pixel can be derived with a least-square sine fitting algorithm and the software "Matlab". Then, the estimated data of ψ are substituted into the special equations derived from Fresnel's equations, and the two-dimensional refractive index distribution of the GRIN lens can be obtained. Because of its common-path optical configuration, this method has both merits of the common-path interferometry and the heterodyne interferometry. In addition, the phases can be measured without reference signals. The validity of this method is demonstrated.

*eternalsea.eo93g@nctu.edu.tw; phone +886-3-573-1951; fax +886-3-571-6631

Modeling Aspects in Optical Metrology II, edited by Harald Bosse, Bernd Bodermann, Richard M. Silver,
Proc. of SPIE Vol. 7390, 73900G · © 2009 SPIE · CCC code: 0277-786X/09/$18 · doi: 10.1117/12.827319

2. PRINCIPLE

2.1 The optical configuration and the phase of interference signal

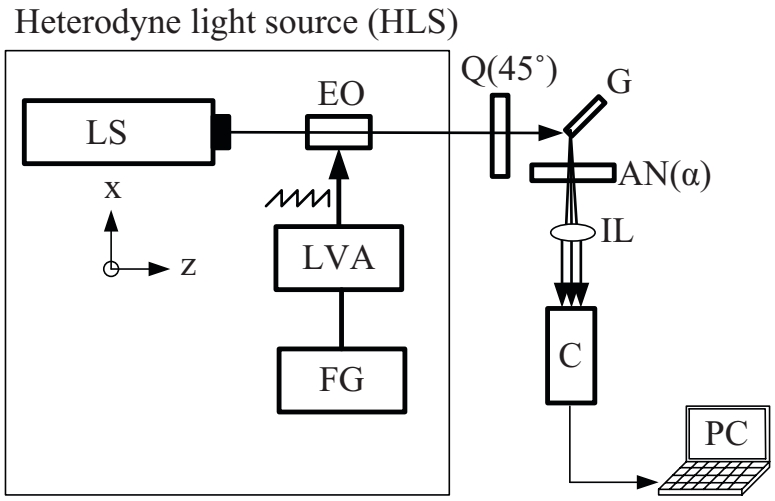

Fig. 1. The optical configuration of this method. LS: laser source; EO: electro-optic modulator; FG: function generator; LVA: linear voltage amplifier; Q: quarter-wave plate; G: GRIN lens; AN: analyzer; IL: imaging lens; C: CMOS camera; PC: personal computer.

The optical configuration of this method is shown in Fig. 1. A heterodyne light source (HLS) [10], which consists of a laser source (LS), an electro-optic modulator (EO), a function generator (FG) and a linear voltage amplifier (LVA), is used in this method. For convenience, the z-axis is chosen along the light propagation direction and the y-axis is along the vertical direction. If the light beam coming from the light source LS is linearly polarized at 45° with respect to the x-axis, the frequency of the light beam is f_0, and the phase difference between the s- and the p-polarizations is Γ, then the Jones vector of the light beam can be written as

$$\begin{aligned} E_{HLS} &= EO(\Gamma)\cdot E_0 \\ &= \begin{pmatrix} e^{i\frac{\Gamma}{2}} & 0 \\ 0 & e^{-i\frac{\Gamma}{2}} \end{pmatrix} \frac{1}{\sqrt{2}} \begin{pmatrix} 1 \\ 1 \end{pmatrix} e^{i2\pi f_0 t} \\ &= \frac{1}{\sqrt{2}} \begin{pmatrix} e^{i\frac{\Gamma}{2}} \\ e^{-i\frac{\Gamma}{2}} \end{pmatrix} e^{i2\pi f_0 t}, \end{aligned} \tag{1}$$

where E_0 is the Jones vector of the LS and $EO(\Gamma)$ is the Jones matrix of the EO. After the light beam passes through a quarter-wave plate (Q) with the fast axis at 45° with respect to the x-axis, the Jones vector becomes

$$\begin{aligned} E &= Q(45°)\cdot E_{HLS} \\ &= \frac{1}{\sqrt{2}} \begin{pmatrix} 1 & i \\ i & 1 \end{pmatrix} \frac{1}{\sqrt{2}} \begin{pmatrix} e^{i\frac{\Gamma}{2}} \\ e^{-i\frac{\Gamma}{2}} \end{pmatrix} e^{i2\pi f_0 t} \end{aligned}$$

$$= \frac{1}{2}\begin{pmatrix}1\\ i\end{pmatrix} e^{\frac{i\Gamma}{2}} e^{i2\pi f_0 t} + \frac{1}{2}\begin{pmatrix}i\\ 1\end{pmatrix} e^{-\frac{i\Gamma}{2}} e^{i2\pi f_0 t}, \tag{2}$$

where the $Q(45°)$ is the Jones matrix of the Q. From Eq. (2), it can be seen that there is a phase difference Γ between the right- and the left- circular polarizations. Next, the light is incident on the tested GRIN lens (G) with refractive index distribution *n(x,y)* at an angle θ, as shown in Fig. 1. The reflected light passes through an analyzer (AN) with the transmission axis at α° with respect to the x-axis and an imaging lens (L), finally it enters a CMOS camera (C). The electric field of the light beam at the C can be represented as

$$\begin{aligned} E_c &= AN(\alpha)\cdot G\cdot E \\ &= \begin{pmatrix}\cos^2\alpha & \sin\alpha\cos\alpha\\ \sin\alpha\cos\alpha & \sin^2\alpha\end{pmatrix}\begin{pmatrix}r_p & 0\\ 0 & r_s\end{pmatrix}\frac{1}{2}\begin{pmatrix}e^{\frac{i\Gamma}{2}} + ie^{-\frac{i\Gamma}{2}}\\ ie^{\frac{i\Gamma}{2}} + e^{-\frac{i\Gamma}{2}}\end{pmatrix} e^{i2\pi f_0 t} \\ &= \frac{1}{2}\begin{pmatrix} r_{\mathrm{p}}\cos^2\alpha\left(e^{\frac{i\Gamma}{2}} + ie^{-\frac{i\Gamma}{2}}\right) + r_{\mathrm{s}}\sin\alpha\cos\alpha\left(ie^{\frac{i\Gamma}{2}} + e^{-\frac{i\Gamma}{2}}\right)\\ r_{\mathrm{p}}\sin\alpha\cos\alpha\left(e^{\frac{i\Gamma}{2}} + ie^{-\frac{i\Gamma}{2}}\right) + r_{\mathrm{s}}\sin^2\alpha\left(ie^{\frac{i\Gamma}{2}} + e^{-\frac{i\Gamma}{2}}\right)\end{pmatrix} e^{i2\pi f_0 t}, \end{aligned} \tag{3}$$

where $AN(\alpha)$ and G are the Jones matrices of the AN and the G, respectively; r_{p} and r_s are the amplitude reflectance coefficients of the p- and the s- polarization of the G. They can be written as

$$r_p = \frac{n\cos\theta - \frac{\sqrt{n^2 - \sin^2\theta}}{n}}{n\cos\theta + \frac{\sqrt{n^2 - \sin^2\theta}}{n}}, \tag{4}$$

and

$$r_s = \frac{\cos\theta - \sqrt{n^2 - \sin^2\theta}}{\cos\theta + \sqrt{n^2 - \sin^2\theta}}. \tag{5}$$

Hence, the intensity of the interference signal on the C can be calculated by the square of the electric field E_c and it can be written as

$$\begin{aligned} I &= |E_c|^2 \\ &= I_0(1 + \gamma\cos(\Gamma + \phi - \frac{\pi}{2})) \\ &= I_0(1 + \gamma\cos(\Gamma + \phi')), \end{aligned} \tag{6}$$

where I_0 and γ can be represented as

$$I_0 = \frac{1}{2}\left(r_p^2\cos^2\alpha + r_s^2\sin^2\alpha\right), \tag{7}$$

and

$$\gamma = 1, \tag{8}$$

respectively; where $\phi' = \phi - \frac{\pi}{2}$ and ϕ can be written as

$$\phi(x,y) = \tan^{-1}\left(\frac{\left(\sin^2\theta - n^2\cos^2\theta\right)\sin 2\alpha}{\left(2\sin^4\theta - \sin^2\theta + n^2\cos^2\theta\right)\cos 2\alpha - 2\sin^2\theta\cos\theta\sqrt{n^2 - \sin^2\theta}} \right). \tag{9}$$

Finally, Eq. (9) can be rewritten as

$$n(x,y) = \sqrt{\frac{-B + \sqrt{B^2 - 4AC}}{2A}}, \tag{10}$$

where

$$A = \left(\frac{\cos\theta\cos 2\alpha\tan\phi + \cos\theta\sin 2\alpha}{2\sin^2\theta} \right)^2, \tag{11}$$

$$B = \left(\frac{\cos 2\theta\cos 2\alpha\tan\phi - \sin 2\alpha}{\cos\theta} \right)\left(\frac{\cos\theta\cos 2\alpha\tan\phi + \cos\theta\sin 2\alpha}{2\sin^2\theta} \right) - \tan^2\phi, \tag{12}$$

and

$$C = \left(\frac{\cos 2\theta\cos 2\alpha\tan\phi - \sin 2\alpha}{2\cos\theta} + \sin^2\theta\tan^2\phi \right)^2. \tag{13}$$

It is obvious from Eq. (10) that the two-dimensional refractive index distribution *n(x,y)* of the G can be calculated with the measurement of phase $\phi(x,y)$ under the experimental conditions in which θ and α are specified.

2.2 Phase estimation [11]

The EO in the HLS is driven by an external sawtooth voltage signal with a moderate dc bias coming from the FG and the VLA. If the frequency and the amplitude of the sawtooth voltage signal are f and V, respectively, then the phase difference Γ between the s- and the p- polarizations can be given as [10]

$$\begin{aligned} \Gamma &= \frac{\pi V}{V_\pi} \\ &= \frac{\pi}{V_\pi}\left[2Vf\left(t - \frac{m}{f} \right) - V \right] \\ &= 2\pi f \frac{V}{V_\pi}\left(t - \frac{m}{f} \right) - \phi_0, \end{aligned} \tag{14}$$

where V_π is the half-wave voltage of the EO; m is an integer and its magnitude is $\frac{m}{f} \le t \le \frac{(m+1)}{f}$; $\phi_0 = \frac{\pi V}{V_\pi}$ is the characteristic phase. If n interference intensities recorded by any pixel at time $t_1, t_2 \ldots t_n$ are $I_1, I_2 \ldots I_n$, respectively, then we have

$$\begin{aligned} I(t_k) &= I_0\left(1 + \gamma\cos(\Gamma + \phi')\right) \\ &= I_0\left(1 + \gamma\cos(2\pi f \frac{V}{V_\pi}\left(t_k - \frac{m}{f} \right) - \phi_0 + \phi') \right) \end{aligned}$$

$$= I_0\left[\left(1+\gamma\cos(2\pi f\frac{V}{V_\pi}\left(t_k-\frac{m}{f}\right)+\psi)\right)\cdot rect(t_k f-\frac{1}{2})\right]*\sum_{i=0}^{n-1}\delta\left(t_k-\frac{i}{f}\right), \qquad (15)$$

where $\psi=\phi'-\phi_0$; f_s is the frame rate of the C; n is the maximum value of m； the symbol *rect*( ) and * represent the rectangle function and the convolution operator, respectively. It can be seen that the period of the cosine function in Eq. (15) is $\frac{V_\pi T}{V}$; both the window width of the rectangle function and the period of the windowed delta function are T. If $V<V_\pi$ occurs, the frequency of the cosine function is less than *f*. *I(t)* becomes a group of periodic sinusoidal segments, and each segment has an initial phase ψ, as shown in Fig. 2. If both the window width of the rectangle function and the period of the windowed function are lengthened to $T+\Delta t$, Eq. (15) can be modified as

$$I'(t)=I_0\left[\left(1+\gamma\cos(2\pi f\frac{V}{V_\pi}\left(t-\frac{m}{f}\right)+\psi)\right)\cdot rect(\frac{ft}{1+f\Delta t}-\frac{1}{2})\right]*\sum_{i=0}^{n-1}\delta\left(t-i(\frac{1}{f}+\Delta t)\right), \qquad (16)$$

where $\Delta t=\frac{V_\pi}{Vf}-\frac{1}{f}$. Consequently, the interference signal is modified to a continuous sinusoidal signal by adding the time difference Δt. If ψ can be measured accurately, the data of ϕ can be calculated under the condition that V and V_π are specified.

The symbol ● shown in Fig. 2 represents the intensities recorded by the C. The theoretical starting points of sinusoidal segments in the time axis are at local extreme positions, which can be determined by operating the second order differential on Eq. (15). They are always different from the sampled starting points of the discrete digital signals taken by the C. The sampled starting point of every segment may not be at the same relative position and the theoretical starting point of the associated segment. To determine an "optimum segment" whose sampled starting point is located closest to the theoretical starting point of the associated segment, let P_m and C_m be the time of sampled starting point and the time comparing point of the mth segment, respectively; and the initial condition $C_1=P_1$ exists. Then, the conditions

$$C_{m+1}=C_m+T, \quad \text{if } P_{m+1}>C_m+T \qquad (17)$$

and

$$C_{m+1}=P_{m+1}, \quad \text{if } P_{m+1}\le C_m+T \qquad (18)$$

should be applied iteratively until the optimum segment has been identified, where m=1, 2, 3,…, n. If $m = i$ is the optimal segment, then the origin of the time axis is so shifted that the condition $P_i=0$ is given and it can be written as

$$I_c'(t)=I_0\left[\left(1+\gamma\cos(2\pi f\frac{V}{V_\pi}t+\psi)\right)\cdot rect(\frac{V}{V_\pi}ft-\frac{1}{2})\right]\cdot\sum_{g=0}^{h-1}\delta\left(t-\frac{g}{f_s}\right) \qquad (19)$$

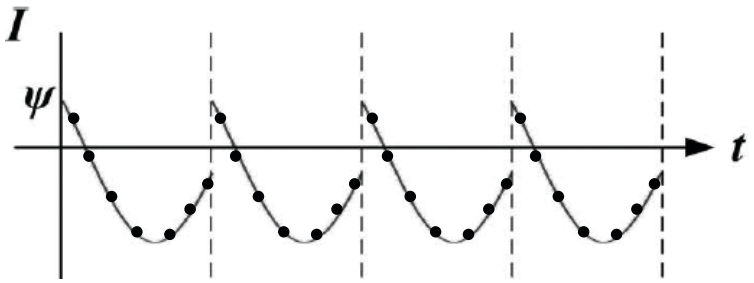

Fig. 2. The sampled interference signals as $V<V_\pi$.

where *g* is a positive integer; *h* is the *h*th sampled point in *i*th segment. Next, the time difference $\Delta t = \frac{V_\pi - V}{Vf}$ is inserted into any two consecutive segments where *m*>*i*. Consequently, this continuously sinusoidal signal can be represented as

$$I_c(t_k) = I_0\left(1+\gamma\cos(2\pi\frac{V}{V_\pi T}t_k+\psi)\right). \tag{20}$$

Then, Eq. (20) is processed by using the three parameter sine wave fitting [12, 13] to get the phase data ψ and the fitted equation has the form of

$$\begin{aligned} I'(t_k) &= A_0\cos(2\pi ft_k)+B_0\sin(2\pi ft_k)+C_0 \\ &= \sqrt{A_0^{\,2}+B_0^{\,2}}\cos(2\pi ft_k+\psi), \end{aligned} \tag{21}$$

where

$$\psi = \tan^{-1}\left(-\frac{B_0}{A_0}\right). \tag{22}$$

A_0, B_0 and C_0 are constants. According to the least square method [12], they can be obtained by minimizing the sum of the quadratic errors

$$S = \sum_{k=1}^{n}\left[I_c(t_k)-I'(t_k)\right]^2. \tag{23}$$

Partially differentiating Eq. (23) with respect to A_0, B_0 and C_0 and then equating the derivatives to zero gives a linear system of three equations

$$D_0 x = y, \tag{24}$$

where

$$D_0 = \begin{pmatrix} \sum_{k=1}^{n}\cos(2\pi ft_k) & \sum_{k=1}^{n}\cos^2(2\pi ft_k) & \sum_{k=1}^{n}\cos(2\pi ft_k)\sin(2\pi ft_k) \\ \sum_{k=1}^{n}\sin(2\pi ft_k) & \sum_{k=1}^{n}\cos(2\pi ft_k)\sin(2\pi ft_k) & \sum_{k=1}^{n}\sin^2(2\pi ft_k) \\ n & \sum_{k=1}^{n}\cos(2\pi ft_k) & \sum_{k=1}^{n}\sin(2\pi ft_k) \end{pmatrix}, \tag{25}$$

$$x = \begin{pmatrix} A_0 \\ B_0 \\ C_0 \end{pmatrix}, \tag{26}$$

and

$$y = \begin{pmatrix} \sum_{k=1}^{n} I_{kg} \cos(2\pi f t_k) \\ \sum_{k=1}^{n} I_{kg} \sin(2\pi f t_k) \\ \sum_{k=1}^{n} I_{kg} \end{pmatrix}. \tag{27}$$

Consequently, we have

$$x = D_0^{-1} y, \tag{28}$$

where D_0^{-1} means the inverse matrix of D_o. From Eq. (25), A_0 and B_0 can be calculated. They are substituted into Eq. (22) and the data of ψ can be estimated. Finally, the measured phases are obtained by calculating $\phi = \psi + \phi_0 + \frac{\pi}{2}$. If these processes are applied to other pixels, then their phases can be obtained similarly. The two-dimensional phase distribution can be obtained.

3. EXPERIMENTS AND RESULTS

In order to show the feasibility, a GRIN lens (AC Photonics, Inc./ALC-18) with diameter 1.8mm was tested. An He-Ne laser with 632.8 nm wavelength, a CMOS camera (Baslar/A504k) with 370×600 pixels and 8-bit gray levels, and an imaging lens (Schnider/21-036942) were used under the conditions $f_s = 450Hz$, $\theta = 45°$ and $\alpha = 10°$. The EO (New Focus/Model 4002) with $V_{\lambda/2} = 148\ V$ was driven by a sawtooth wave voltage with $V = 120V$ and $f = 15Hz$. The interferograms were sent to a personal computer, and they were analyzed with the software Matlab (MathWorks Inc.). The measured results of $\phi(x, y)$ were substituted into Eq. (10), the two-dimensional refractive index distribution $n(x, y)$ could be calculated and the results are shown in Fig. 3(a). For clarity, one-dimensional refractive index distribution along the dotted line in Fig. 3(a) was calculated and its profile is shown in Fig. 3(b).

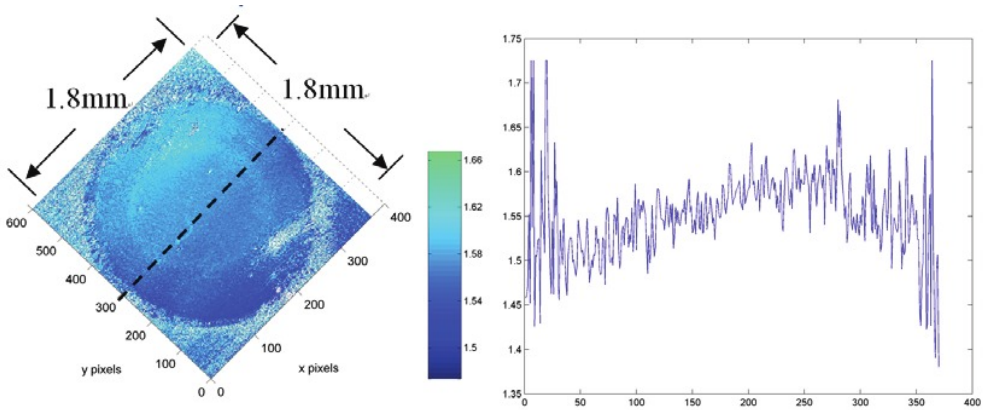

(a) (b)

Fig. 3. (a) The two-dimensional refractive index distribution of the GRIN lens. (b) One-dimensional refractive index profile along the dotted line in Fig. 3(a).

4. DISCUSSION

From Eq. (10), we have

$$\triangle n = \left|\frac{\partial n}{\partial \phi}\right| \delta\phi \,, \tag{29}$$

where $\triangle n$ and $\delta\phi$ are the errors in n and ϕ, respectively. The phase error $\delta\phi$ may be caused by the sampling error $\delta\phi_1$ [14], the polarization mixing error $\delta\phi_2$ [15, 16] and the characteristic phase error $\delta\phi_3$ coming from the ambient turbulance. To decrease the effect coming from the instability of frequency difference f, we choose the condition $f / f_s = 30$ in our tests and $\delta\phi_1$ can be minimized to 0.036° [14]. The extinction ratio of the AN (Newport Inc.) is 1×10^{-3}, $\delta\phi_2$ can be reduced to 0.027° [15]. The errors in V and V_π directly introduce a systematic error $\delta\phi_3$ to the characteristic phase ϕ_0. The resolution of V from the FG is $\Delta V_1 = 0.016V$. Also V_π can be measured [17], and its error is estimated $\Delta V_2 = 0.015V$. Hence the maximum error of ϕ_0 can be estimated and expressed as $\delta\phi_3 = \phi_{\max} \cdot \left[\left(\Delta V_1 / V\right)^2 + \left(\Delta V_2 / V\right)^2 \right]^{1/2} \approx 0.03°$, where $\phi_{\max} = 180°$ is the maximum possible phase. So, the total experimental phase error $\delta\phi = \delta\phi_1 + \delta\phi_2 + \delta\phi_3 \approx 0.093°$. Substituting the experimental conditions $\theta = 45°$, $\alpha = 10°$ and $\delta\phi = 0.093°$ into Eq. (29), the relation curve of $\triangle n$ versus n can be calculated and shown in Fig. 4. It can be seen that $\triangle n$ depends on n.

5. CONCLUSION

An alternative method for measuring the two-dimensional refractive index distribution of a GRIN lens has been presented in this paper. After a linearly polarized light passes through the EO and the Q, it is incident on a GRIN lens. The reflected light propagates through the A, and then the interference signal can be obtained. The special equations to estimate the phase of the interferometric signal can be derived by using Fresnel equations. The full-field heterodyne interference signals are taken by a fast CMOS camera. The associated phase of each pixel can be derived with a least-square sine fitting algorithm. Then, the measured data are substituted into the special equations derived previously. Finally, the two-dimensional refractive index distribution of the GRIN lens can be obtained. Because of the common-path optical configuration, it has both merits of the common-path interferometry and the heterodyne interferometry. The validity of this method has been demonstrated.

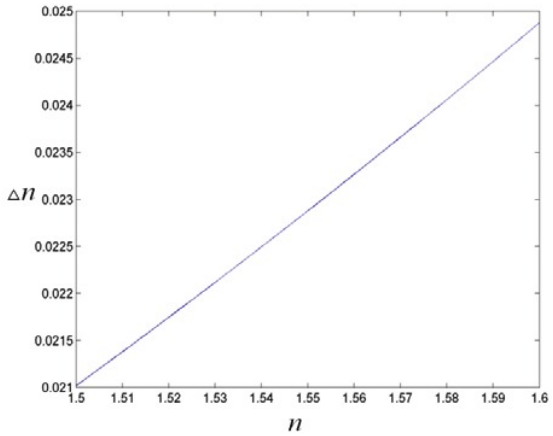

Fig. 4. The relation curve of $\triangle n$ versus n.

REFERENCES

[1] Chao, Y. F. and Lee, K. Y., "Index profile of radial gradient index lens measured by imaging ellipsometric technique," Jap. Jour. Appl. Opt. 44, 1111-1114 (2005).

[2] Liu, Z., Dong, X., Chen, Q., Yin, C., Xu, Y. and Zheng, Y., "Nondestructive measurement of an optical fiber refractive-index profile by a transmitted-light differential interference contact microscope," Appl. Opt. 43, 1485-1492 (2004).

[3] Vazquez, D., Acosta, E., Smith, G. and Garner, L., "Tomographic method for measurement of the radiant refractive index of the crystalline lens. II The rotationally symmetrical lens," Opt. Soc. Am. A 23, 2551- 2565 (2006).

[4] Ray, M., Sarkar, S. K., Basuray, A., and SoodBiswas, N., "Measurement of refractive index profile of GRIN glasses," SPIE 4417, 483- 488(2001).

[5] Conde, R. and Depeursinge, C., "Refractive index profile and geometry measurements in multicore fibres," Pure Appl. Opt. 5, 269–274 (1996).

[6] Born, M. and Wolf, E., Principles of optics, 7th ed., Pergamon, Oxford, UK , p.40 (1999).

[7] Malacara, D., Optical shop testing, 3rd ed., John Wiley, USA, p. 547 (2007).

[8] Yariv, A. and Yeh, P., Optical waves in crystals, John Wiley & Sons, New York, p. 276 (1984).

[9] Rastogi, P. K., Optical measurement techniques and applications, Artech House, Boston, p. 101 (1997).

[10] Su, D. C., Chiu, M. H. and Chen, C. D., "Simple two frequency laser" Prec. Eng. 18, 161-163 (1996).

[11] Chen, Y. L. and Su, D. C., "Method for determining full-field absolute phases in the common-path heterodyne interferometer with an electro-optic modulator", Appl. Opt. 47, 6518-6523 (2008).

[12] IEEE Standard for terminology and test methods for analog-to-digital converters IEEE Std. 1241-2000 25-29 (2000).

[13] Farrell, C. T. and Player, M. A., "Phase-step insensitive algorithms for phase-shifting interferometry", Meas. Sci. Technol. 5, 648-652 (1994).

[14] Jian, Z. C., Chen, Y. L., Hsieh, H. C., Hsieh, P. J. and Su, D. C., "An optimal condition for the full-field heterodyne interferometry", Opt. Eng. 46, 115604 (2007).

[15] Hou, W. and Wilkening, G., "Investigation and compensation of the nonlinearity of heterodyne interferometers" Prec. Eng. 14, 91-98 (1992).

[16] De Freitas, J. M. and Player, M. A., "Importance of rotational beam alignment in the generation of second harmonic errors in laser heterodyne interferometry" Meas. Sci. Technol. 4, 1173-1176 (1993).

[17] Dou, Q., Ma, H. J., Chen, Z., Cao, K. and Zhang, T., "Study on measurement of linear electro-optic coefficient of a minute irregular octanhedron cBN wafer," Opt. Laser Technol. 39, 647-651 (2007).